

Redox Transformations and Transport of Cesium and Iodine (−1, 0, +5) in Oxidizing and Reducing Zones of a Sand and Gravel Aquifer

PATRICIA M. FOX,* DOUGLAS B. KENT,
AND JAMES A. DAVIS

U.S. Geological Survey, 345 Middlefield Road, MS 496, Menlo Park, California 94025

Received September 21, 2009. Revised manuscript received January 15, 2010. Accepted January 29, 2010.

Tracer tests were performed in distinct biogeochemical zones of a sand and gravel aquifer in Cape Cod, MA, to study the redox chemistry (I) and transport (Cs, I) of cesium and iodine in a field setting. Injection of iodide (I^-) into an oxic zone of the aquifer resulted in oxidation of I^- to molecular iodine (I_2) and iodate (IO_3^-) over transport distances of several meters. Oxidation is attributed to Mn-oxides present in the sediment. Transport of injected IO_3^- and Cs^+ was retarded in the mildly acidic oxic zone, with retardation factors of 1.6–1.8 for IO_3^- and 2.3–4.4 for Cs. Cs retardation was likely due to cation exchange reactions. Injection of IO_3^- into a Fe-reducing zone of the aquifer resulted in rapid and complete reduction to I^- within 3 m of transport. The nonconservative behavior of Cs and I observed during the tracer tests underscores the necessity of taking the redox chemistry of I as well as sorption properties of I species and Cs into account when predicting transport of radionuclides (e.g., ^{129}I and ^{137}Cs) in the environment.

Introduction

Radioactive isotopes of cesium (^{137}Cs) and iodine (^{131}I and ^{129}I) are environmental contaminants derived from nuclear fission reactions. These radioisotopes have been released to the environment during nuclear accidents such as Chernobyl and fallout from weapons testing and are important constituents of nuclear waste (1–4). The United States faces the challenge of safely disposing of high-level and low-level radioactive waste, often for long periods of time. It is important to understand the geochemistry of these elements in groundwater systems in order to protect human and environmental health. While laboratory experiments can provide valuable information on reactions of these elements with sediments, field experiments give direct information on the transport of contaminants in more complex natural systems and are an invaluable tool for developing models to predict contaminant transport.

Iodine is commonly found as iodide (I^-), iodate (IO_3^-), and organic I in natural waters at concentrations of 10^{-9} to 10^{-6} M (5–7). Iodide and iodate are thought to react little in groundwater systems. However, research in marine sediments indicates that I^- may be oxidized by manganese oxides,

nitrate, or other sediment constituents to I_2 or IO_3^- (8, 9). Transport of molecular iodine (I_2) may be retarded because of uptake by sediment organic matter (10–12) and volatilization (13, 14). It has been recently demonstrated that the Mn-oxide mineral birnessite oxidizes I^- to I_2 and IO_3^- under mildly acidic to neutral pH conditions (15, 16). Under reducing conditions, IO_3^- may be reduced to I^- via abiotic and biotic pathways (17–21).

Cesium is commonly found as the monovalent cation Cs^+ and is known to sorb strongly to sediments via cation exchange (22, 23). Cs sorption has been successfully described using a two site model, including a strong site and a weak site corresponding to the frayed edge sites (FES) and planar sites of phyllosilicates, respectively (22, 24). Several researchers have noted that a fraction of the Cs is irreversibly sorbed (22, 25).

In this study, field transport experiments in distinct geochemical zones were performed in a shallow sand and gravel aquifer in order to determine dominant chemical reactions influencing the transport of cesium and iodine, including oxidation and reduction reactions influencing iodine species under oxygenated and iron-reducing conditions and the influence of chemical conditions on adsorption of iodine species and cesium.

Materials and Methods

Site Description. Field experiments were performed in a shallow unconfined sand and gravel aquifer located in western Cape Cod, MA (26). Discharge of treated sewage at the Massachusetts Military Reservation from 1938 to 1995 resulted in a plume of sewage-contaminated groundwater characterized by various biogeochemical zones (27–29). The plume is surrounded by oxic, mildly acidic groundwater with low dissolved salt concentrations. Iron reduction is the dominant microbial process in the core of the plume, which has near neutral pH values (30). Dissolved organic carbon concentrations were 0.7–0.8 mg/L in the oxic zone and 0.7–1.0 mg/L in the Fe-reducing zone. Sediments have less than 0.1% organic carbon (31). Quartz comprises greater than 90% of the sediments throughout the study area. Adsorption properties are controlled by coatings of micro- and nanocrystalline iron oxyhydroxides and aluminosilicates (31–33). Reductively extractable Mn concentrations of sediments from site F168 are 0.73–2.04 $\mu\text{mol/g}$ (34).

Field experiments were conducted in the Fe-reducing zone (site F625) (30) and the pristine, oxic zone of the aquifer (site F168) (35) (Figure S1 of the Supporting Information). Each site has an array of multilevel samplers (MLS) for collection of breakthrough curves at different depths and distances downgradient. Background water chemistry at the injection wells used for the three field experiments is shown in Table 1.

Tracer Test Injections and Sampling. Three tracer tests commenced in August 2006: (1) injection of CsI and NaBr into an oxygenated zone of the aquifer at F168 M17-02 (oxic I^-), (2) injection of CsBr and $NaIO_3$ into an oxygenated zone at F168 M17-08 (oxic IO_3^-), and (3) injection of CsBr and $NaIO_3$ into a Fe-reducing zone of the aquifer at F625 M02-09 (anoxic IO_3^-). Injection conditions are shown in Table 2. The two injections into well F168 M17 were vertically separated by 1.5 m, and no mixing of the tracer clouds was observed. Groundwater for injections was collected from MLS within 5–10 m and from the same depth interval as the injection ports. Tracer salts were mixed into the groundwater before injecting. For the anoxic injection, introduction of dissolved oxygen was minimized by collecting groundwater in a gas

* Corresponding author phone: (650) 329-4480; e-mail: pfox@usgs.gov.

TABLE 1. Background Chemistry at Injection Wells Used for Transport Experiments

well and port	DO (μM)	Ca (mol/L)	K (mol/L)	Mg (mol/L)	Na (mol/L)	Mn (mol/L)	Fe (mol/L)
F168 M17-02	140	9.2×10^{-6}	1.3×10^{-5}	2.9×10^{-5}	2.4×10^{-4}	5.3×10^{-7}	bdl ^a
F168 M17-08	230	1.7×10^{-5}	1.5×10^{-5}	3.7×10^{-5}	2.3×10^{-4}	2.6×10^{-7}	bdl ^a
F625 M02-09	bdl ^a	2.0×10^{-4}	8.5×10^{-5}	5.9×10^{-5}	9.0×10^{-4}	2.6×10^{-6}	2.1×10^{-4}
well and port	pH	Alk (meq/L)	P (mol/L)	Si (mol/L)	Cl ⁻ (mol/L)	SO ₄ ²⁻ (mol/L)	NH ₄ ⁺ (mol/L)
F168 M17-02	4.7	bdl ^a	bdl ^a	1.1×10^{-4}	2.5×10^{-4}	7.1×10^{-5}	bdl ^a
F168 M17-08	5.1	0.005	bdl ^a	1.4×10^{-4}	2.0×10^{-4}	7.1×10^{-5}	bdl ^a
F625 M02-09	6.6	0.950	9.7×10^{-5}	2.3×10^{-4}	4.9×10^{-4}	1.4×10^{-4}	5.8×10^{-6}

^a bdl = below detection limit.

TABLE 2. Tracer Test Characteristics and Injected Tracer Concentrations

	oxic I ⁻	oxic IO ₃ ⁻	anoxic IO ₃ ⁻
injection Port	F168 M17-02	F168 M17-08	F625 M02-09
injection altitude (m to sea level)	8.21	6.75	1.02
volume (L)	360	380	180
Cs (mM)	1.1	1.0	1.0
I (mM)	1.1	1.0	1.0
Br (mM)	1.1	1.0	1.0
Na (mM)	1.3	1.3	1.9
pH	4.7	5.2	6.5

impermeable bag thoroughly purged with N₂. Tracers were dissolved in deionized water that had been boiled for at least 20 min to remove oxygen and then mixed into groundwater as described elsewhere (36).

Groundwater samples were collected from MLS ports at distances of 1–4 m for breakthrough data. Using a peristaltic

pump, 150 mL of groundwater was purged from each MLS port before collecting water samples for in-field (pH, conductivity) and laboratory analyses (0.45 μm filtered). Samples collected for iodine determination were kept in the dark and refrigerated until analysis (within 4 h) by spectrophotometry. Samples collected for Br and other anions were

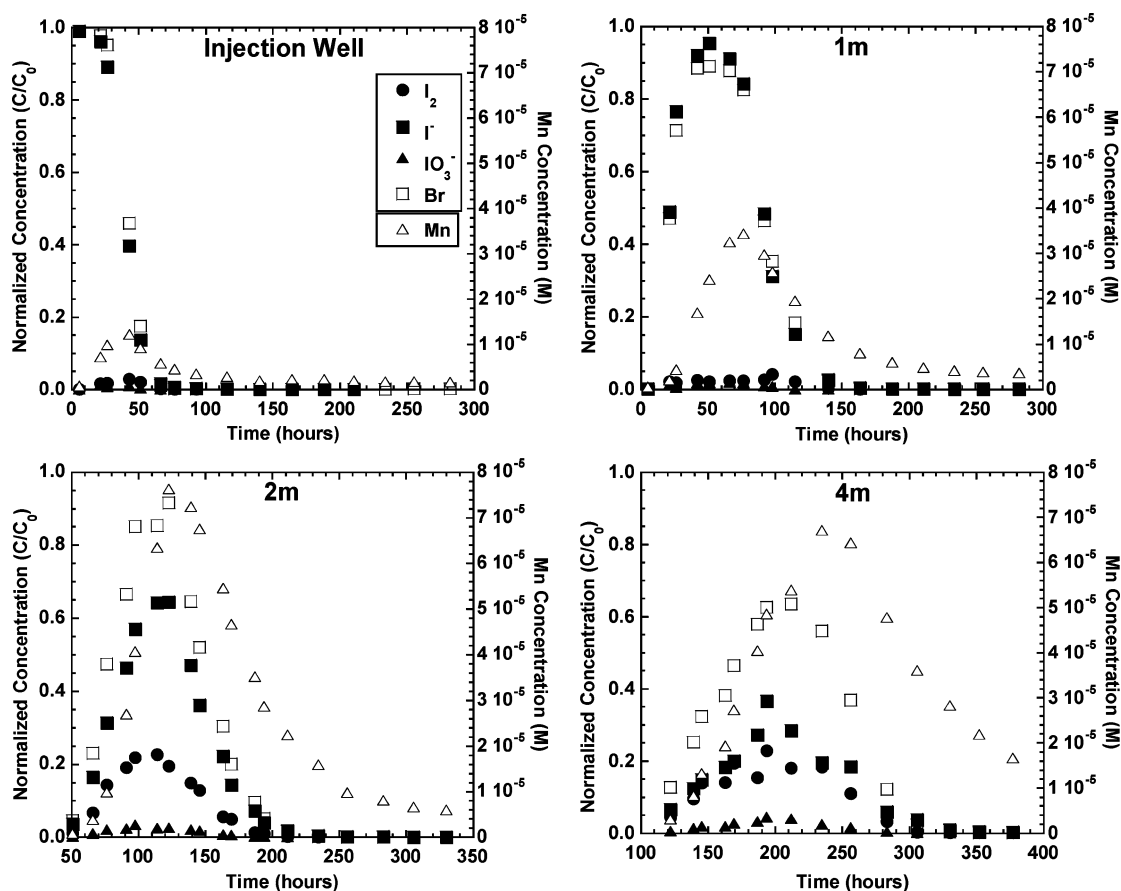


FIGURE 1. Breakthrough curves showing Br⁻, I⁻, I₂, IO₃⁻, and dissolved Mn concentrations at various distances downgradient of the injection well in the oxic I⁻ tracer test. All Br and I species concentrations are normalized to the injection concentration.

TABLE 3. Transport Parameters for Br, Iodine species, and Cs

distance (m)	velocity (m/day) ^a	R_{it}^b		attenuation factor (A_i) ^c			
		total I	Cs	I ⁻	I ₂	IO ₃ ⁻	total I
oxic iodide tracer test							
1.0	0.40	1.0	2.3	1.03	0.04	0.02	1.08
2.0	0.41	1.0	2.7	0.71	0.25	0.03	0.99
4.0	0.48	1.0	4.0	0.47	0.32	0.05	0.84
oxic iodate tracer test							
1.0	0.25	1.6	2.9	— ^d	—	1.23	1.23
2.0	0.26	1.7	3.3	—	—	1.22	1.22
4.0	0.28	1.8	4.4	—	—	1.16	1.16
anoxic iodate tracer test							
3.0	0.36	1.0	—	—	0.81	ND	0.81

^a Average groundwater velocity calculated from Br travel times. ^b Retardation factor calculated from average travel time for the given tracer divided by that of Br. ^c Attenuation factor (inverse) calculated from the area under the curve for the tracer divided by that of Br. ^d Species not detected.

frozen. Br was measured using either ICP-MS (for samples containing I⁻ or I₂) or a colorimetric method (for samples containing only IO₃⁻). A subset of Br samples was analyzed by both methods in order to verify agreement between the two methods. Selected samples were also analyzed by ion chromatography for nitrate, phosphate, chloride, sulfate, and ammonium. Samples collected for elemental analysis by ICP-AES (Na, K, Mg, Ca, Mn, Fe, Si, P) and ICP-MS (Cs) were acidified to pH 2 with trace metal grade nitric acid.

Iodine species were measured colorimetrically on three separate samples: (1) active iodine, (2) active iodine + iodide, and (3) iodate. Active iodine includes elemental I₂ and its hydrolysis products, HOI and OI⁻, and in the presence of excess iodide, I₃⁻. Active iodine will be referred to as “iodine”

or “I₂” hereafter. Active iodine and iodide were determined using the leuco-crystal violet method, in which a citric acid buffer solution (pH 3.8) and leuco crystal violet indicator solution are added to each sample, and absorbance is measured at 592 nm (37). Addition of oxone (KHSO₅) oxidizes iodide to iodine, and iodide can be determined by difference. Iodate was determined by adding an excess of iodide and sulfamic acid to produce I₃⁻ and measuring absorbance at 351 nm (38). The iodate concentrations were corrected for the presence of I₃⁻ and Fe(II), which imparts a slight yellow color in the untreated sample. This correction never exceeded 0.004 mM. The validity of this correction technique was verified using standard additions. Samples were diluted to achieve concentrations of 2–30 μM for I⁻ and I₂ and 1–10

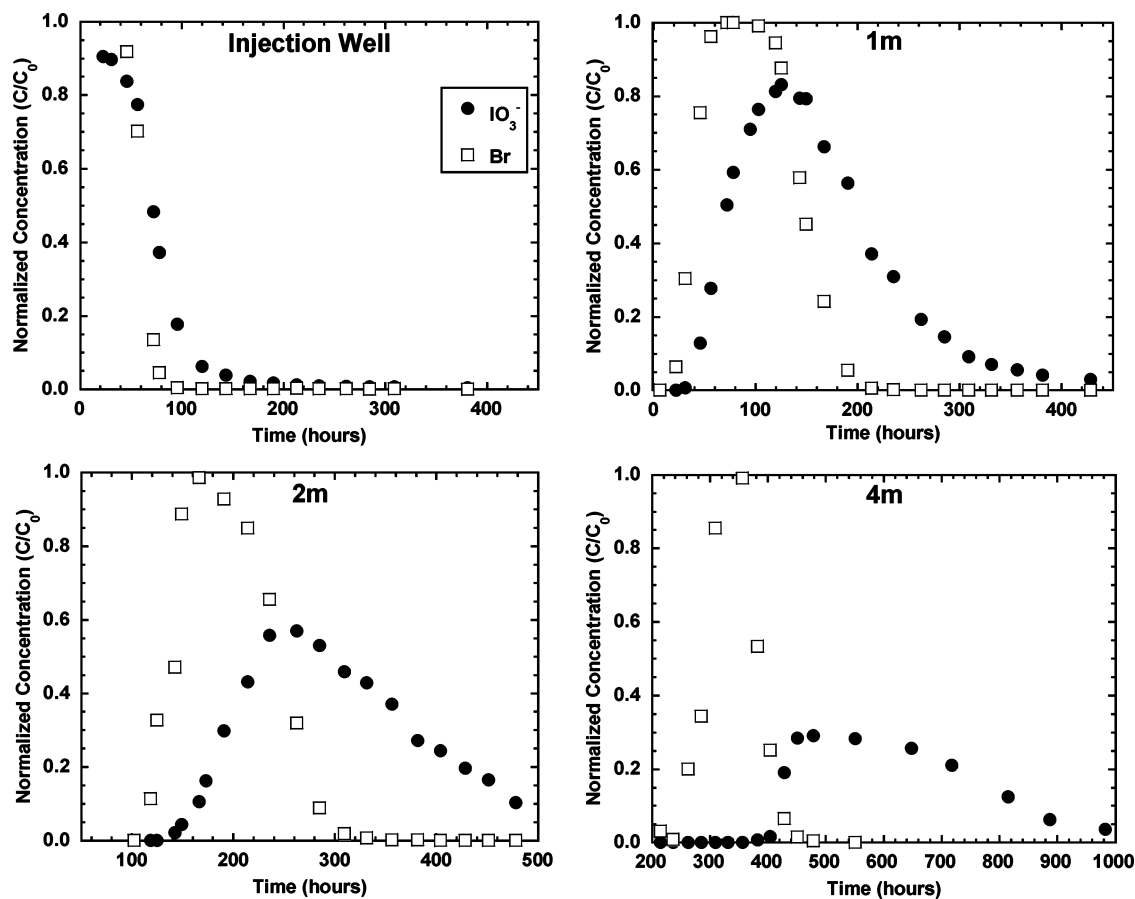


FIGURE 2. Iodate and Br breakthrough curves at various distances downgradient from the injection well in the oxic iodate tracer test. All concentrations are normalized to the injection concentration. Note the different time scales for different transport distances.

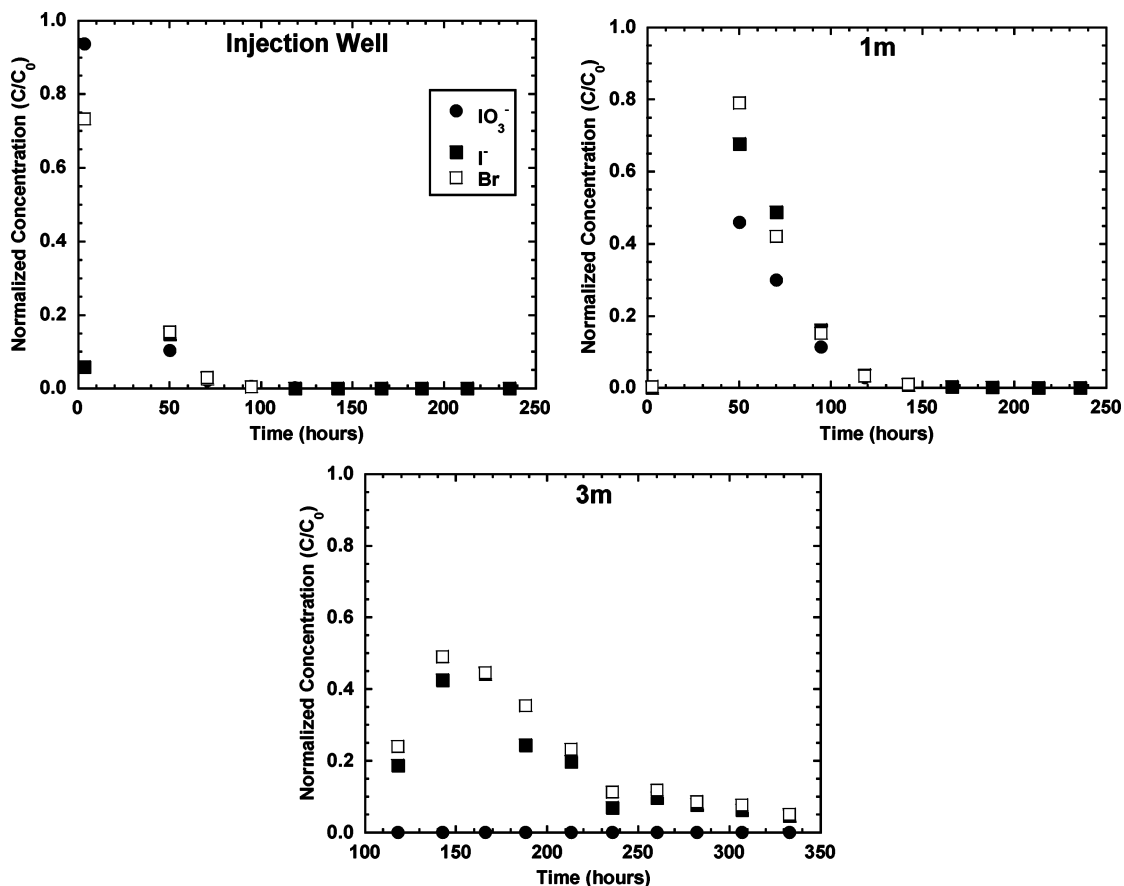


FIGURE 3. Br^- , IO_3^- , and I^- breakthrough curves at various distances downgradient from the injection well for the anoxic iodate injection. Concentrations are normalized to the injection concentrations.

μM for IO_3^- , over which range absorbance was linear. Organic iodine forms are not detected using these spectroscopic methods.

Results and Discussion

Iodide Oxidation in the Oxidic Tracer Test. Iodide was oxidized to I_2 and IO_3^- over 1–4 m of transport during the oxidic tracer test (Figure 1). Extent of oxidation was quantified by calculating (inverse) attenuation factors (A_f), where the area under the breakthrough curve for each species is divided by the area under the Br^- breakthrough curve, using normalized concentrations (39). Decreases in the A_f value for I^- showed that minimal oxidation occurred over the first 1 m of transport, but after 2 m, 29% of the injected I^- had been oxidized, primarily to I_2 (Table 3). After 4 m, approximately 32% had been oxidized to I_2 and 5% to IO_3^- (Table 3).

On the basis of thermodynamic considerations, there are several possible iodide oxidants: dissolved O_2 , NO_3^- , and Mn and Fe oxides (see Figure 1 in Fox et al. (15) for thermodynamic calculations). However, I^- oxidation by dissolved oxygen is kinetically unfavorable in the absence of a strong oxidant to catalyze the reaction (40) and nitrate concentrations were extremely low ($<1 \mu\text{M}$) in the study area. Iodide oxidation by Mn oxides is favorable up to about pH 7.3, and manganese oxides have been shown to rapidly oxidize a variety of inorganic contaminants including As(III), Cr(III), and $\text{I}(-1)$ (12, 15, 16, 41–43), whereas I^- oxidation by FeOOH is only favorable under acidic conditions (15). Previously, we demonstrated that birnessite oxidizes I^- in a 2-step reaction to I_2 and IO_3^- and that the oxidation proceeds faster at lower pH (15).

Laboratory experiments demonstrated that sediments collected throughout the study area oxidized As(III) to As(V) most probably because of Mn oxides on the sediments (34).

Sediment samples collected closest to the tracer test location (F168-15) contained $2.04 \mu\text{mol/g}$ of reductively extractable Mn (34). At a solid–liquid ratio of 4000 g/L in the aquifer (porosity = 0.4 and solid-phase density = 2.65 g/cm^3), there is approximately 8.2 mM of Mn available for I^- oxidation. Assuming reduction of Mn(IV) to Mn(II), oxidation of 1 mM I^- to I^0 would require 0.5 mM of Mn(IV) and oxidation of I^- to IO_3^- would require 3 mM of Mn(IV). The low apparent yield of IO_3^- suggests that the oxidation of I_2 to IO_3^- was rate-limited, given the apparent excess availability of Mn(IV). The observed increase in Mn concentrations associated with breakthrough of the injected tracers (Figure 1), provides further evidence that Mn oxides were the electron acceptors responsible for I^- oxidation. No increase in dissolved Fe concentrations was observed. Dissolved Mn concentrations increased with transport distance as more I^- was oxidized, reaching up to $7.6 \times 10^{-5} \text{ M}$ at 2 m downgradient. Clearly, the observed increase in Mn was not stoichiometrically proportional to the amount of I^- oxidized. It has been shown that nonstoichiometric increases in Mn^{2+} upon oxidation results from Mn adsorption (41). Thus, the observed dissolved Mn was only a fraction of the total Mn^{2+} produced during the reaction of Mn oxides with I^- . The observed retardation of Mn provides further evidence of Mn^{2+} adsorption under the prevailing chemical conditions. No such increase in Mn concentrations was observed in the oxidic tracer test in which IO_3^- was injected (Figure S5 of the Supporting Information), demonstrating that increases in Mn concentrations cannot be attributed to ion exchange reactions releasing sorbed Mn^{2+} .

Calculated retardation factors (R_f) for total I were 1.0 (Table 3), indicating that neither I^- nor I_2 was extensively sorbed. R_f was calculated from the ratios of the average travel times for the solute of interest (total I in this case) divided by the

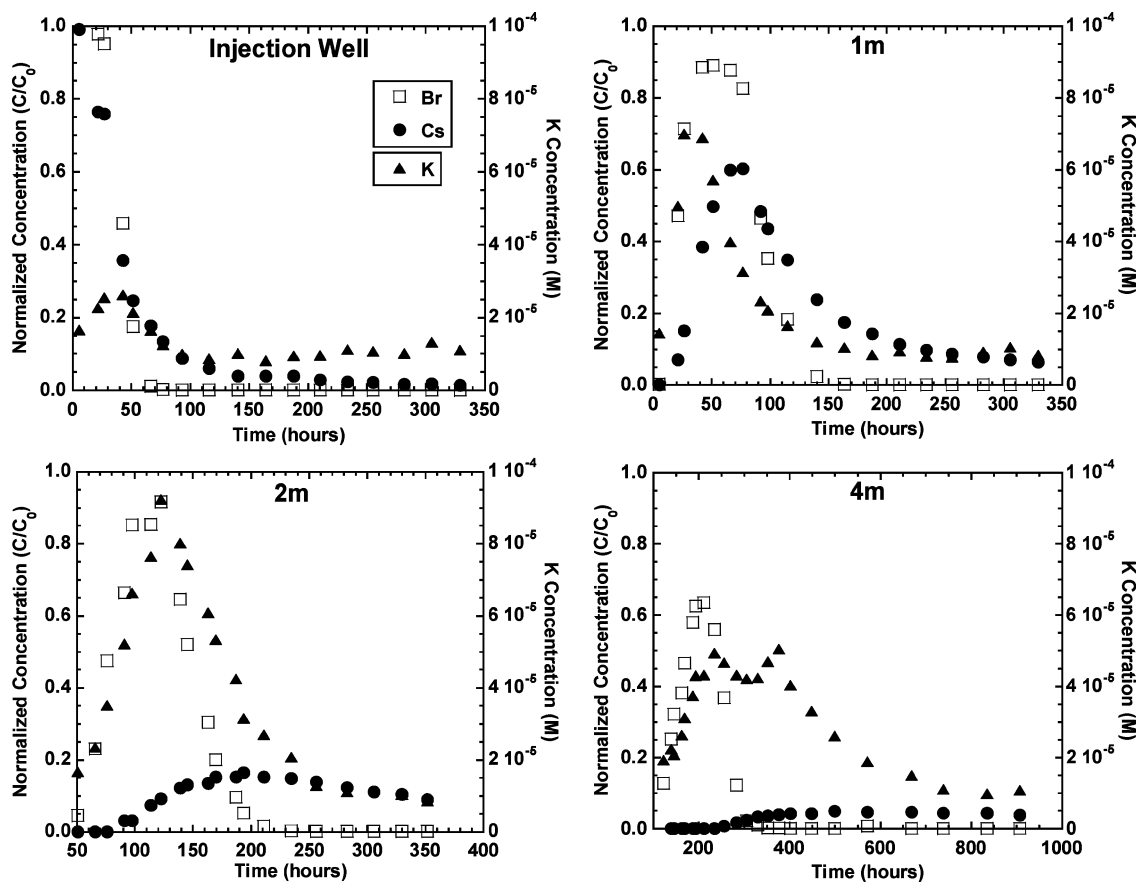


FIGURE 4. Breakthrough curves showing Cs, Br, and dissolved K at various distances downgradient from the injection well in the oxidic iodide tracer test. Cs and Br concentrations are normalized to the concentrations in the injectate. Note the different time scales in each panel.

average travel time for Br (39). Although no retardation of I₂ was observed in this study, it is important to note that sediments from the study area have <0.1% organic carbon (31). Uptake of I₂ by organic matter is well-established (10–12), and one would expect significantly more retardation of I₂ during transport in an aquifer containing higher levels of organic matter. Organic carbon concentrations are often the limiting factor in the formation of organic iodine species (44), and thus, at high iodine concentrations and low organic carbon contents like those in our study area, organic iodine may not be detected.

Attenuation factors for total I (Table 3) over the first 2 m of transport equaled 1.0 within experimental error, indicating no irreversible uptake of I species. After 4 m of transport, A_f for total I was 0.84. Uncertainties in attenuation factors for nonadsorbing injected tracers, detailed elsewhere, are in the range of 0.12–0.2 (45). Contributing factors to uncertainty are analytical errors (which increase near the detection limit), lack of resolution during peak breakthrough, and failure to capture the leading and trailing edges of the curve. The most likely cause of irreversible uptake should be formation of organic I (10–12, 44). Thus, minimal loss of I would be expected on the basis of the low concentration of organic matter in the study area.

Iodate Sorption in the Oxidic Iodate Tracer Test. Iodate was significantly retarded when injected into the oxidic region of the aquifer (Figure 2). After 4 m of transport, significant spreading of IO₃⁻ resulted in a peak concentration that was 29% of the injected concentration. The R_f calculated for IO₃⁻ was 1.6–1.8 at transport distances of 1–4 m (Table 3). Retardation and significant tailing indicates that iodate sorbs to the sediments under these conditions. The apparent lack of retardation of iodate produced during the oxidic I⁻ experi-

ment may have resulted from production of iodate near the leading edge of the tracer cloud (Figure 1). Other researchers have observed that iodate exhibits higher sorption and is more retarded than iodide in laboratory batch and column studies (18, 46). Couture and Seitz (46) observed pH dependent IO₃⁻ sorption to hematite over a wide range of concentrations (10⁻¹² to 10⁻³ M) and suggested that specific sorption occurred on a single sorption site, similar to that of phosphate on hematite. The constant A_f of 1.2 with transport distance (Table 3) suggests that sorption of IO₃⁻ on these sediments is reversible on the time scale of transport.

Iodate Reduction in the Anoxic Iodate Tracer Test. Rapid reduction of iodate to iodide was observed when iodate was injected into the iron-reducing region of the aquifer (Figure 3). Iodide concentrations exceeded those of iodate during breakthrough 1 m downgradient of the injection, and iodate reduction was complete after 3 m of transport. No significant retardation was observed (Table 3). In contrast to the oxidation of iodide, no I₂ was detected during the anoxic tracer test, suggesting that I₂ is not a stable intermediate during reduction under these conditions. The mechanism of reduction is unknown, but abiotic and biotic reduction mechanisms have been proposed. Microbially mediated reduction of IO₃⁻ by *Desulfovibrio desulfuricans* and *Shewanella putrefaciens* without significant production of I₂ has been demonstrated (20, 21). Abiotic reduction by various inorganic compounds has been observed or proposed, including Fe²⁺ (dissolved and solid phases), organic matter, dissolved Mn²⁺, and dissolved S²⁻ (8, 18, 20). Neither dissolved S²⁻ nor FeS has been detected in the Fe-reducing zone; however, both Fe²⁺ and Mn²⁺ were present. Dissolved concentrations of Fe (2.07 × 10⁻⁴ M) and Mn (2.59 × 10⁻⁶ M) represent only a fraction of the available pools of Fe²⁺

and Mn^{2+} because significant sorption of these metals is expected at near-neutral pH values. Perturbations in Fe concentrations during breakthrough 1 m downgradient suggest possible involvement of Fe in the reduction of iodate (Figure S6 of the Supporting Information).

Cesium Retardation and Attenuation. Extensive retardation and tailing of Cs was observed in all three tracer tests. In the oxic zone (Figure 4 and Figure S2 of the Supporting Information), retardation and spreading after 4 m of transport resulted in a decrease in the maximum Cs concentration to 5% of the injected concentration. In the Fe-reducing zone, no Cs was detected beyond 1 m, likely due in part to a significantly lower mass of Cs used in the anoxic injection than in either of the oxic injections. R_f values of 2.3–4.4 are calculated for Cs transport in the oxic zone. A R_f value could not be calculated for the anoxic IO_3^- test because of incomplete breakthrough curves. The R_f values increased with transport distance for Cs in the oxic tests. This observation can be explained by the existence of multiple binding sites on the sediment with different binding affinities such as the two site (strong and weak site) model invoked to describe Cs sorption on Hanford sediments (22, 23). Pulses of increased K, Ca, and Mg concentrations preceded Cs breakthrough (Figure 4 and Figures S2–S6 of the Supporting Information), which suggest that Cs uptake occurred via cation exchange. This hypothesis is consistent with laboratory observations of Cs sorption to sediments (22, 23). Zachara et al. (22) demonstrated that competition with Cs for binding sites on Hanford sediment was in the order of $\text{K} \gg \text{Na} \geq \text{Ca}$. The double peaks in K likely result from a difference in binding affinities of Cs and Na injected with iodide/iodate and bromide.

Other researchers have reported that 10%–30% of Cs is irreversibly sorbed at loading levels of 10^{-7} to 10^{-5} mol/g (22, 25). Continued transport of Cs downgradient in our experiments suggests largely reversible sorption of Cs (Figure 4). This difference may result from the extremely low collapsible clay mineral content of the Cape Cod aquifer sediments (30) as compared to that of the micaceous Hanford sediments, where irreversible sorption is explained as a migration of Cs into the interlayers of clay minerals (22, 25).

Implications. Both iodine species and cesium can undergo reactions with sediments that influence their transport in groundwater. Under oxic conditions, iodide was oxidized to I_2 and IO_3^- , probably by Mn oxides in the sediments. Assuming that the rate of I^- oxidation by MnO_2 is first-order with respect to I^- , as demonstrated in experimental studies (15), one would expect the fraction of oxidized iodine produced to be similar at the lower iodine concentrations more typically observed (10^{-9} to 10^{-6} M). The production of I_2 may be important in organic-rich systems (e.g., the Savannah River Site), particularly at ambient iodine concentrations, because I_2 strongly binds to organic material. Rapid reduction of iodate to iodide under Fe-reducing conditions indicates that iodide should be the dominant species in anoxic groundwater. Cs was retarded extensively, likely due to cation exchange. In aquifers with elevated concentrations of collapsible clay minerals, more extensive irreversible sorption than was observed during our experiments may occur. These results demonstrate the importance of taking redox transformations into consideration when predicting iodine transport in aquifers and other sediment–water systems.

Acknowledgments

We would like to thank Denis LeBlanc, Luke Parsons, and Deborah Stoliker of the USGS for invaluable assistance in the field, and Jennifer Joye for help with sample analysis. The Nuclear Regulatory Commission provided financial support through Interagency Agreement RES-03-006.

Supporting Information Available

Map of the field site, plots of Cs breakthrough during the oxic iodate and anoxic iodate tracer tests, and plots of major ion concentrations during all three tests. This information is available free of charge via the Internet at <http://pubs.acs.org/>.

Literature Cited

- (1) Filipovic-Vincekovic, N.; Barisic, D.; Masic, N.; Lulic, S. Distribution of fallout radionuclides through soil surface layer. *J. Radioanal. Nucl. Chem.* **1991**, *148* (1), 53–62.
- (2) Blagoeva, R.; Zikovskiy, L. Geographic and vertical distribution of Cs-137 in soils in Canada. *J. Environ. Radioact.* **1995**, *27* (3), 269–274.
- (3) Oktay, S. D.; Santschi, P. H.; Moran, J. E.; Sharma, P. The ^{129}I iodine bomb pulse recorded in Mississippi River Delta sediments: Results from isotopes of I, Pu, Cs, Pb, and C. *Geochim. Cosmochim. Acta* **2000**, *64* (6), 989–996.
- (4) Rao, U.; Fehn, U. Sources and reservoirs of anthropogenic iodine-129 in western New York. *Geochim. Cosmochim. Acta* **1999**, *63* (13/14), 1927–1938.
- (5) Oktay, S. D.; Santschi, P. H.; Moran, J. E.; Sharma, P. ^{129}I and ^{127}I transport in the Mississippi River. *Environ. Sci. Technol.* **2001**, *35* (22), 4470–4476.
- (6) Luther, G. W., III; Ferdelman, T.; Culberson, C. H.; Kostka, J.; Wu, J. Iodine chemistry in the water column of the Chesapeake Bay: Evidence for organic iodine forms. *Estuarine, Coastal Shelf Sci.* **1991**, *32* (3), 267–279.
- (7) Schwehr, K.; Santschi, P. H.; Elmore, D. The dissolved organic iodine species of the isotopic ratio of $^{129}\text{I}/^{127}\text{I}$: A novel tool for tracing terrestrial organic carbon in the estuarine surface waters of Galveston Bay, Texas. *Limnol. Oceanogr.: Methods* **2005**, *3*, 326–337.
- (8) Anschutz, P.; Sundby, B.; Lefrancois, L.; Luther, G. W.; Mucci, A. Interactions between metal oxides and species of nitrogen and iodine in bioturbated marine sediments. *Geochim. Cosmochim. Acta* **2000**, *64* (16), 2751–2763.
- (9) Truesdale, V. W.; Watts, S. F.; Rendell, A. R. On the possibility of iodide oxidation in the near-surface of the Black Sea and its implications to iodine in the general ocean. *Deep-Sea Res., Part I* **2001**, *48* (11), 2397–2412.
- (10) Warner, J. A.; Casey, W. H.; Dahlgren, R. A. Interaction kinetics of $\text{I}_2(\text{aq})$ with substituted phenols and humic substances. *Environ. Sci. Technol.* **2000**, *34* (15), 3180–3185.
- (11) Sheppard, M. I.; Thibault, D. H.; McMurry, J.; Smith, P. A. Factors affecting the soil sorption of iodine. *Water, Air, Soil Pollut.* **1995**, *83* (1–2), 51–67.
- (12) Gallard, H.; Allard, S.; Nicolau, R.; von Gunten, U.; Croue, J. P. Formation of iodinated organic compounds by oxidation of iodide-containing waters with manganese dioxide. *Environ. Sci. Technol.* **2009**, *43* (18), 7003–7009.
- (13) Keppler, F.; Eiden, R.; Niedan, V.; Pracht, J.; Schöler, J. F. Halocarbons produced by natural oxidation processes during degradation of organic matter. *Nature* **2000**, *403*, 298–301.
- (14) Kuepper, F. C.; Carpenter, L. J.; McFiggans, G. B.; Palmer, C. J.; Waite, T. J.; Boneberg, E. M.; Woitsch, S.; Weiller, M.; Abela, R.; Grolimund, D.; Potin, P.; Butler, A.; Luther III, G. W.; Kroneck, P. M. H.; Meyer-Klaucke, W.; Feiters, M. C. Iodide accumulation provides kelp with an inorganic antioxidant impacting atmospheric chemistry. *Proc. Nat. Acad. Sci. U.S.A.* **2008**, *105*, 6954–6958.
- (15) Fox, P. M.; Davis, J. A.; Luther, G. W., III. The kinetics of iodide oxidation by the manganese oxide mineral birnessite. *Geochim. Cosmochim. Acta* **2009**, *73*(10), 2850–2861.
- (16) Allard, S.; von Gunten, U.; Sahli, E.; Nicolau, R.; Gallard, H. Oxidation of iodide and iodine on birnessite ($\delta\text{-MnO}_2$) in the pH range 4–8. *Water Res.* **2009**, *43* (14), 3417–3426.
- (17) Fuhrmann, M.; Bajt, S.; Schoonen, M. A. A. Sorption of iodine on minerals investigated by X-ray absorption near edge structure (XANES) and ^{129}I tracer sorption experiments. *Appl. Geochem.* **1998**, *13* (2), 127–141.
- (18) Hu, Q.; Zhao, P.; Moran, J. E.; Seaman, J. C. Sorption and transport of iodine species in sediments from the Savannah River and Hanford Sites. *J. Contam. Hydrol.* **2005**, *78* (3), 185–205.
- (19) Yamaguchi, N.; Nakano, M.; Tanida, H.; Fujiwara, H.; Kihou, N. Redox reaction of iodine in paddy soil investigated by field observation and the I K-edge XANES fingerprinting method. *J. Environ. Radioact.* **2006**, *86*, 212–226.

- (20) Councell, T. B.; Landa, E. R.; Lovley, D. R. Microbial reduction of iodate. *Water, Air, Soil Pollut.* **1997**, *100* (1–2), 99–106.
- (21) Farrenkopf, A. M.; Dollhopf, M. E.; Chadhain, S. N.; Luther, G. W.; Nealson, K. H. Reduction of iodate in seawater during Arabian Sea shipboard incubations and in laboratory cultures of the marine bacterium *Shewanella putrefaciens* strain MR-4. *Mar. Chem.* **1997**, *57* (3–4), 347–354.
- (22) Zachara, J. M.; Smith, S. C.; Liu, C.; McKinley, J. P.; Serne, R. J.; Gassman, P. L. Sorption of Cs⁺ to micaceous subsurface sediments from the Hanford site, USA. *Geochim. Cosmochim. Acta* **2002**, *66*, 193–211.
- (23) Ainsworth, C. C.; Zachara, J. M.; Wagnon, K.; McKinley, S.; Liu, C.; Smith, S. C.; Schaef, H. T.; Gassman, P. L. Impact of highly basic solutions on sorption of Cs⁺ to subsurface sediments from the Hanford site, USA. *Geochim. Cosmochim. Acta* **2005**, *69* (20), 4787–4800.
- (24) Poinssot, C.; Baeyens, B.; Bradbury, M. H. Experimental and modelling studies of caesium sorption on illite. *Geochim. Cosmochim. Acta* **1999**, *63* (19/20), 3217–3227.
- (25) Comans, R. N. J.; Haller, M.; de Preter, P. Sorption of cesium on illite: Non-equilibrium behaviour and reversibility. *Geochim. Cosmochim. Acta* **1991**, *55* (2), 433–440.
- (26) LeBlanc, D. R.; Garabedian, S. P.; Hess, K. M.; Gelhar, L. W.; Quadri, R. D.; Stollenwerk, K. G.; Wood, W. W. Large-scale natural-gradient tracer test in sand and gravel, Cape Cod, Massachusetts. 1. Experimental design and observed tracer movement. *Water Resour. Res.* **1991**, *27* (5), 895–910.
- (27) Kent, D. B.; Davis, J. A.; Anderson, L. C. D.; Rea, B. A.; Waite, T. D. Transport of chromium and selenium in the suboxic zone of a shallow aquifer: Influence of redox and adsorption reactions. *Water Resour. Res.* **1994**, *30* (4), 1099–1114.
- (28) LeBlanc, D. R. *Sewage Plume in a Sand and Gravel Aquifer, Cape Cod, Massachusetts*; U. S. Geol. Survey Water Supply Paper 2218; 1984, p 28.
- (29) Repert, D. A.; Barber, L. B.; Hess, K. M.; Keefe, S. H.; Kent, D. B.; LeBlanc, D. R.; Smith, R. L. Long-term natural attenuation of carbon and nitrogen within a groundwater plume after removal of the treated wastewater source. *Environ. Sci. Technol.* **2006**, *40* (4), 1154–1162.
- (30) Höhn, R.; Isenbeck-Schröter, M.; Kent, D. B.; Davis, J. A.; Jakobsen, R.; Jann, S. V.; Niedan, V.; Scholz, C.; Stadler, S.; Tretner, A. Tracer test with As(V) under variable redox conditions controlling arsenic transport in the presence of elevated ferrous iron concentrations. *J. Contam. Hydrol.* **2006**, *88* (1–2), 36–54.
- (31) Barber, L. B.; Thurman, E. M.; Runnells, D. D. Geochemical heterogeneity in a sand and gravel aquifer: Effect of sediment mineralogy and particle size on the sorption of chlorobenzenes. *J. Contam. Hydrol.* **1992**, *9* (1–2), 35–54.
- (32) Coston, J. A.; Fuller, C. C.; Davis, J. A. Pb²⁺ and Zn²⁺ adsorption by a natural aluminum- and iron-bearing surface coating on an aquifer sand. *Geochim. Cosmochim. Acta* **1995**, *59* (17), 3535–3547.
- (33) Davis, J. A.; Coston, J. A.; Kent, D. B.; Fuller, C. C. Application of the surface complexation concept to complex mineral assemblages. *Environ. Sci. Technol.* **1998**, *32* (19), 2820–2828.
- (34) Amirbahman, A.; Kent, D. B.; Curtis, G. P.; Davis, J. A. Kinetics of sorption and abiotic oxidation of arsenic(III) by aquifer materials. *Geochim. Cosmochim. Acta* **2006**, *70* (3), 533–547.
- (35) Kent, D. B.; Davis, J. A.; Anderson, L. C. D.; Rea, B. A. Transport of chromium and selenium in a pristine sand and gravel aquifer: Role of adsorption processes. *Water Resour. Res.* **1995**, *31* (4), 1041–1050.
- (36) Smith, R. L.; Baumgartner, L. K.; Miller, D. N.; Repert, D. A.; Böhlke, J. K. Assessment of nitrification potential in ground water using short term, single-well injection experiments. *Microb. Ecol.* **2006**, *51* (1), 22–35.
- (37) American Public Health Association. *Standard Methods for the Examination of Water and Wastewater*, 18th ed.; American Public Health Association (APHA): Washington, DC, 1992.
- (38) Truesdale, V. W. The automatic determination of iodate and total iodine in seawater. *Mar. Chem.* **1978**, *6*, 253–273.
- (39) Roberts, P. V.; Goltz, M. N.; Dackay, D. M. A natural gradient experiment on solute transport in a sand aquifer. 3. Retardation estimates and mass balances for organic solutes. *Water Resour. Res.* **1986**, *22* (13), 2047–2058.
- (40) Luther, III., G. W.; Wu, J.; Cullen, J. Redox Chemistry of Iodine in Seawater: Frontier Molecular Orbital Theory Considerations. In *Aquatic Chemistry: Interfacial and Interspecies Processes*; Advances in Chemistry Series; Huang, C. P., O'Melia, C. R., Morgan, J. J., Eds.; American Chemical Society: Washington, DC, 1995; Vol. 244, pp 135–155.
- (41) Scott, M. J.; Morgan, J. J. Reactions at oxide surfaces. 1. Oxidation of As(III) by synthetic birnessite. *Environ. Sci. Technol.* **1995**, *29* (8), 1898–1905.
- (42) Manning, B. A.; Fendorf, S. E.; Bostick, B.; Suarez, D. D. Arsenic(III) oxidation and arsenic(V) adsorption reactions on synthetic birnessite. *Environ. Sci. Technol.* **2002**, *36* (5), 976–981.
- (43) Fendorf, S. E.; Zasoski, R. J. Chromium(III) oxidation by delta-MnO₂. 1. Characterization. *Environ. Sci. Technol.* **1992**, *26* (1), 79–85.
- (44) Schwehr, K. A.; Santschi, P. H.; Kaplan, D. I.; Yeager, C. M.; Brinkmeyer, R. Organo-iodine formation in soils and aquifer sediments at ambient concentrations. *Environ. Sci. Technol.* **2009**, *43* (19), 7258–7264.
- (45) Kent, D. B.; Davis, J. A.; Anderson, L. C. D.; Rea, B. A.; Coston, J. A. Effect of adsorbed metal ions on the transport of Zn- and Ni-EDTA complexes in a sand and gravel aquifer. *Geochim. Cosmochim. Acta* **2002**, *66* (17), 3017–3036.
- (46) Couture, R. A.; Seitz, M. G. Sorption of anions of iodine by iron oxides and kaolinite. *Nucl. Chem. Waste Manage.* **1983**, *4* (4), 301–306.

ES902865S